

## Article

# Synthesis, Characterization and Fabrication of Copper Nanoparticles Embedded Non-Perfluorinated Kraton Based Ionic Polymer Metal Composite (IPMC) Actuator

Mohammad Luqman <sup>1,\*</sup>, Arfat Anis <sup>2,\*</sup>, Hamid M. Shaikh <sup>2</sup>, Saeed M. Al-Zahrani <sup>2</sup> and Mohammad Asif Alam <sup>3</sup>

<sup>1</sup> Department of Chemical Engineering, College of Engineering, Taibah University, 4430, Yanbu 46421, Saudi Arabia

<sup>2</sup> SABIC Polymer Research Centre, Department of Chemical Engineering, King Saud University, P.O. Box 800, Riyadh 11421, Saudi Arabia; hamshaikh@ksu.edu.sa (H.M.S.); sahrani@ksu.edu.sa (S.M.A.-Z.)

<sup>3</sup> Center of Excellence for Research in Engineering Materials (CEREM), King Saud University, P.O. Box 800, Riyadh 11421, Saudi Arabia; moalam@ksu.edu.sa

\* Correspondence: luqman@taibahu.edu.sa (M.L.); aarfat@ksu.edu.sa (A.A.)

**Abstract:** Recently, cost-effective ionic polymer metal composite (IPMC) membranes coated with novel metals (viz., Ag, Au, or Pt) have exhibited excellent bending actuation performance, which was electrically stimulated. Herein, we have developed an IPMC membrane of highly cost-effective Kraton (KR) fabricated by incorporating Copper nanoparticles (CuNPs). It was then coated with Pt-metal using a solution casting process. The developed IPMC membrane (KR-CuNPs-Pt) was characterized using Fourier-transform infrared (FTIR) spectroscopy, Transmission electron microscopy (TEM), and X-ray diffraction (XRD) techniques. Further, ionic exchange capacity (IEC), the proton conductivity (PC), and water uptake/loss studies have also been performed. Actuation performance was measured using the electromechanical techniques. The actuation force of ca. 0.343 mN and displacement of ca. 18 mm at 4 VDC indicate that the developed membrane may serve as an alternative to the highly expensive commercialized IPMC actuators based on perfluorinated polymers. A soft bending actuator in the form of a micro-gripper was also developed.

**Keywords:** ionic polymer metal composite (IPMC); sulfonated; Kraton; platinum; artificial muscle; membrane; robotic actuator; gripper



**Citation:** Luqman, M.; Anis, A.; Shaikh, H.M.; Al-Zahrani, S.M.; Alam, M.A. Synthesis, Characterization and Fabrication of Copper Nanoparticles Embedded Non-Perfluorinated Kraton Based Ionic Polymer Metal Composite (IPMC) Actuator. *Actuators* **2022**, *11*, 183. <https://doi.org/10.3390/act11070183>

Academic Editors: Man Yang and Feilong Zhang

Received: 6 June 2022

Accepted: 29 June 2022

Published: 4 July 2022

**Publisher's Note:** MDPI stays neutral with regard to jurisdictional claims in published maps and institutional affiliations.



**Copyright:** © 2022 by the authors. Licensee MDPI, Basel, Switzerland. This article is an open access article distributed under the terms and conditions of the Creative Commons Attribution (CC BY) license (<https://creativecommons.org/licenses/by/4.0/>).

## 1. Introduction

Polymer-based actuators are one of the most important actuation materials that produce various mechanical responses using numerous external stimuli. One of the common stimulators is electrical energy, which converts electrical energy to mechanical energy [1–3]. A lot of polymeric materials are electrically responsive, including ionic polymer gels (IPGs), ionic polymer metal composites (IPMCs), dielectric elastomers (DEMs), conductive polymers (CPs), and piezoelectric polymers (PEPs), which are widely used in making micro/soft robots and biomimetic artificial muscles [4–8]. IPMC-based actuators are attracting lots of attention these days due to their peculiar properties, including high flexibility, low weight, easy molding into various shapes, low applied voltage, and good bending actuation [9,10]. IPMC-based actuators consist of a polymeric membrane sandwiched between layers of two noble metal conductive electrodes. When a hydrated (solvated) strip of IPMCs is subjected to low positive potential (1–5 V), a fast-bending deformation can be seen towards the anode [10–12] as transportation of hydrated ionic movement occurred inside the strip. Similarly, on changing the polarity of voltage (from positive to negative), the bending occurs in reverse direction. Due to this reason, the bidirectional deflection of the membrane is achieved.

These IPMC membranes may function in air, water, or both mediums [11]. The observed bending by applying potential in IPMCs is due to the presence of mobile cations in ion-exchange materials and the water/solvent molecules from the cathode to the anode area. The accretion and disappearance of the water/solvent molecules through the ionomeric membrane is generally assumed to be one of the important factors responsible for IPMC actuation; related to hydraulic, osmotic, and electrostatic forces. For the practical application of IPMCs, and for their ability towards an excellent bending behavior under very low applied voltages, IPMCs must exhibit several characteristic properties, including high water uptake (WU), low water loss (WL) capacity, high ion exchange capacity (IEC) and proton conductivity (PC), electrical conductivity through smooth and good adhesions of noble metal electrodes [13–17].

The perfluorosulfonic acid (PFSA) based polymers, e.g., Nafion<sup>®</sup>, possess excellent thermomechanical and electrical properties; thus, these PFSA-based membranes find many advanced applications, including separation, energy, and actuations. However, PFSA-based polymers, their membranes are usually very costly, including a few other drawbacks. Thus, there is a significant interest among engineers and scientists in looking for cost-effective alternatives to these membranes. Our group recently developed two IPMC membranes based on, e.g., silicotungstic acid-sulfonated polyvinyl alcohol-polyaniline, and sulfonated poly(ether ether ketone)-polyaniline coated with platinum [3,5]. These membranes showed good actuation performance. Different types of IPMC membranes with a combination of all or a few of these factors, including low to high synthetic convenience, environment friendliness, flexibility, mechanical strength, ion exchange capacity, proton conductivity, water absorption and loss capacities, actuation force, and tip displacement/deflection levels, need to be explored continuously for different soft robotic or biomimetic applications, as different applications may need different materials/characteristics. Thus, the present work, which describes the development of a Kraton-based ionomeric membrane as a novel actuation material, can be treated as an effort in this direction. The sole intention of this study is to provide a cost-effective alternative to very costly commercially available PFSA-based membranes for soft robotic applications.

It is well known that composites of two or more materials have fascinating characteristics and properties that were not usually possible to establish with the individual components. We have selected a non-perfluorinated sulfonated penta-block copolymer known as Kraton as an ion-exchange polymeric material due to the specific characteristics viz., good electromechanical properties, high PC and IEC, large WU capacity, and excellent membrane forming capacity. The prepared membrane was characterized using various techniques such as FTIR spectroscopy, TEM, and XRD technique.

## 2. Materials and Methods

### 2.1. Materials

A non-perfluorinated Kraton [pentablock copolymer poly((t-butyl-styrene)-b-(ethylene-r-propylene)-b-(styrene-r-styrene sulfonate)-b-(ethylene-r-propylene)-b-(t-butyl-styrene) (tBS-EP-SS-EP-tBS)](MD9200) (Nexar Polymer, Houston, TX, USA); hydrochloric acid (HCl-35%), ammonium hydroxide (NH<sub>4</sub>OH-25%); (Merck Specialties Pvt Ltd., Darmstadt, Germany), Sodium borohydride (NaBH<sub>4</sub>) and Tetraamine platinum(II) chloride monohydrate [Pt(NH<sub>3</sub>)<sub>4</sub>Cl<sub>2</sub>·H<sub>2</sub>O (Crystal form)] (Alfa Aesar, Haverhill, MA, USA), copper chloride and sodium oleate (Sigma-Aldrich Chemie Pvt. Ltd., St. Louis, MO, USA), tetrahydrofuran (THF), hexane, and ethanol (Merck, Germany) were used in this study. The purchased analytical grade chemicals and reagents were used as such.

### 2.2. Methods

#### 2.2.1. Instrumentation

An FTIR-ATR spectrometer (Thermo Scientific, Winsford, UK); XRD (Rigaku, miniflex-II, Tokyo, Japan); SEM (JEOL, JSM-6510 LV, Tokyo, Japan); TEM (2100, JEOL, Tokyo, Japan, operated 200 kV); potentiostat/galvanostat (PGSTAT 302 N Autolab, Luzern, Switzerland);

pH meter; magnetic stirrer; digital electronic balance; and an electric air oven were used for drying, measurements, and characterization of the prepared composite membrane.

### 2.2.2. Synthesis of Copper Nanoparticles (CuNPs)

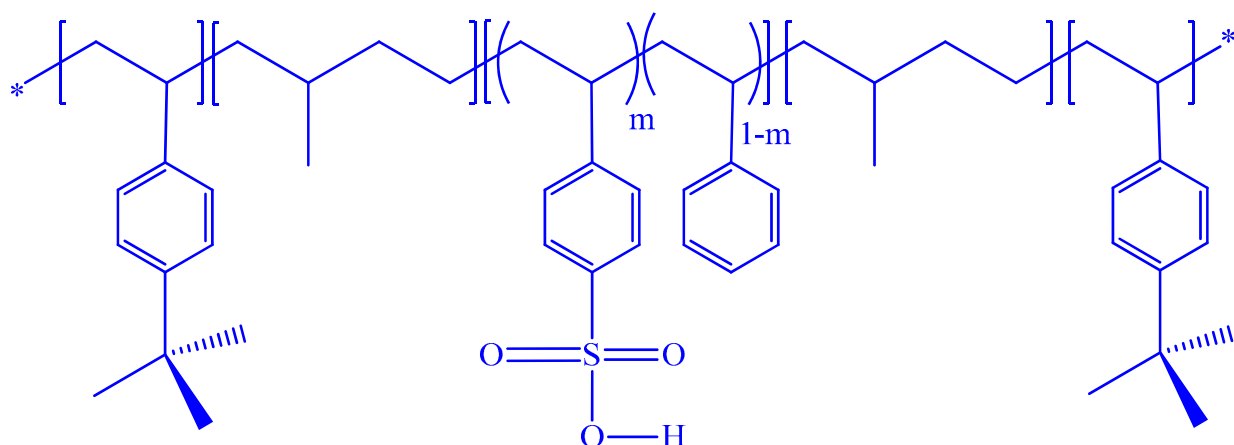
For the preparation of CuNPs, copper chloride (1.08 g) and sodium oleate (3.65 g) were weighed, and a solution of hexane, ethanol, and demineralized water (DMW) was prepared. The weighed materials were mixed into the prepared solution, heated, and refluxed for almost 5 h. The solution was then transferred to a separating funnel to remove the aqueous residues. The obtained complex was washed 3–4 times with DMW and was transferred to a Petri dish to evaporate the solvent residue. Now, the complex (ca. 3.6 g) was mixed with oleic acid (1.14 g) and then dissolved into phenyl ether (20 g) at room temperature. The final obtained solution was heated for about 30 min at 25 °C. A brown precipitate was obtained, confirming the formation of CuNPs. The resulting precipitate was cooled and washed for several minutes with ethanol to remove the solvent and residues. Finally, CuNPs were obtained by centrifugation [18].

### 2.2.3. Characterization of CuNPs

XRD patterns were recorded using a diffractometer (Rigaku, Miniflex-II, Japan). The size of CuNPs was determined using TEM (2100, JEOL, Japan, operated 200 kV) carbon coated copper grid [18].

### 2.2.4. Membrane Fabrication of KR-CuNPs

For the fabrication of the membrane, we prepared a solution by dissolving 4.0 g of KR polymer in 20.0 mL of THF at room temperature with constant stirring up to 8 h. Then, 0.01 gm of prepared CuNPs were transferred into 3 mL of THF and sonicated up to 1 h. Both of the prepared solutions were mixed for the fabrication and again sonicated up to 4 h. After that, the mixture was cast into a petri dish (85 × 15 mm<sup>2</sup>), covered with filter paper for slow evaporation of THF and placed in an oven at room temperature up to 24 h. A drying process was completed and removed with the help of forceps; a membrane of KR-CuNPs was obtained, which was cut into a dimension of 1 × 3 cm<sup>2</sup>. The fabricated membrane was used for further study [19,20]. Scheme 1 describes the structure of KR.



**Scheme 1.** Schematic representation of the chemical structure of Kraton.

### 2.2.5. Chemical Plating

Pt-metal coating at the KR-CuNPs polymer surface was performed using an electroless plating method. The surface of the KR-CuNPs polymer membrane was roughed from both sides with the help of mild sandpaper, and the membrane was cleaned using an ultrasonicator for 10 min. The membrane was then rinsed in HCl (2.0 M) at room temperature (25 ± 1 °C) for 8 h and it was neutralized with demineralized water (DMW). A 4.5 mL of aqueous solution of hydrated Pt(NH<sub>3</sub>)<sub>4</sub>Cl<sub>2</sub> and 1.0 mL of NH<sub>4</sub>OH was mixed and used

in coating the Pt-metal electrode on KR-CuNPs polymer membrane. The membrane was placed for digestion in the reaction chamber at room temperature for 8 h. Now, the prepared membrane was immersed in DMW to release the excess Pt ions from the surface of the exposed membrane. An aqueous solution of  $\text{NaBH}_4$  (1.0 mL) was prepared and used six to eight times dropwise and it was seen that the Pt ions reduced to Pt-metal within an interval of 30 min. An aqueous solution of  $\text{NaBH}_4$  (about 5.0 mL) was prepared and added to the Pt-metal solution with constant stirring for 1.5 h. The prepared membrane was cleaned with DMW and rinsed in a solution of 0.1 M HCl to reduce Pt ions into Pt-metal. The prepared membrane was further kept for drying for 12 h. As the membrane gets hydrated, the cations get diffused towards the electrode, where the material surfaces are kept under an applied electric field. The anions were interconnected as clusters inside the polymer's structure. This provides a channel for the flow of cations towards the electrode. The flow of hydrated ions leads to the bending structure of the membrane towards the anode.

#### 2.2.6. Characterization of the Membrane Actuator

The characteristic properties such as IEC, PC, WU (by mass%), and WL (by mass%) of the KR-CuNPs-Pt IPMC membrane were evaluated similarly to the process reported by Inamuddin et al. [15]. Structural features of this IPMC membrane were characterized using FTIR and XRD. SEM technique was employed to investigate surface and cross-sectional morphologies of the membrane. Their images were captured for the observation of the coating of Pt on the surface of the polymer membrane. EDX analysis of the IPMC membrane was done to show the particle size and distribution of various metals present with focus on Pt metal. For testing the bending performance of the IPMC actuator, electromechanical characterization, including the deflection/displacement of tip and actuation or blocking force, was carried out under a sinusoidal voltage ( $\pm 4$  V).

#### 2.2.7. Ion-Exchange Capacity (IEC)

The strength of  $\text{H}^+$  ions liberated from neutralized salt, commonly known as the IEC (in  $\text{meq}\cdot\text{g}^{-1}$ ), was determined using the standard column method. The dried IPMC membranes (0.25 g) were cut into small pieces and put into  $\text{HNO}_3$  (1.0 M) for 24 h to convert into  $\text{H}^+$  form and were taken out of the solution, washed with DMW, and then was put in an oven for drying at ca.  $45^\circ\text{C}$ . The dried polymer membrane was now in a protonated form that was compressed into a glass column. An eluent, e.g.,  $\text{NaNO}_3$  (1.0 M) was used to elute protons fully from the column, with a flow rate of 0.5 mL/min. A 0.1 M standard NaOH solution was used to titrate the effluent with the help of phenolphthalein as an indicator. The IEC value was calculated using the reported equation [15,16].

$$\text{Ion exchange capacity} = \frac{\text{Volume of NaOH consumed} \times \text{Molarity of NaOH}}{\text{Weight of dry film}} \quad (1)$$

The IEC for the IPMC was found to be ca.  $2.1 \text{ meq}\cdot\text{g}^{-1}$ .

#### 2.2.8. Water Uptake (WU)

The evaluation of WU capacity of the prepared IPMC membranes was performed. For this, the membranes were put into DMW for absorption of water at three different temperatures:  $25 \pm 1^\circ\text{C}$ ,  $45^\circ\text{C}$ , and  $65^\circ\text{C}$  for a period of 24 h. This was done to analyze the effect of temperature and time on WU capacity. Membranes were then taken out of the water at different intervals of time, and the surface of the membrane was cleaned with filter paper to remove traces of water droplets, and then the membranes were weighed. The WU capacity of the membranes was calculated with the help of the following equation [14].

$$\text{WU} = \frac{W_{\text{wet}} - W_{\text{dry}}}{W_{\text{dry}}} \quad (2)$$

where  $W_{\text{wet}}$  and  $W_{\text{dry}}$  are the weights of *wet* and *dry* membranes, respectively.

### 2.2.9. Water Loss (WL)

Based on the water uptake experiment, the KR-CuNPs IPMC membrane was first put in DMW for almost 1 h at  $25 \pm 1$  °C for a maximum water absorption level. The membrane was taken out, and it was weighed again after removing the water droplets from the surface. The WL capacity measurement of the membrane was performed by applying electric potential at a range of 3–6 V for a short interval ranging from 3 to 9 min. It was then calculated using the following formula [15]:

$$\% \text{ WL} = \frac{W_1 - W_2}{W_1} \times 100 \quad (3)$$

where  $W_1$  is the weight of the hydrated membrane and  $W_2$  is the weight of the membrane after applying the electric potential.

### 2.2.10. Proton Conductivity (PC)

PC of a hydrated membrane with dimensions of  $1 \times 3 \text{ cm}^2$  was evaluated at  $25 \pm 1$  °C using an impedance analyzer over a frequency of 100 kHz, which was connected with Autolab 302 N modular potentiostat/galvanostat and an AC perturbation of  $10 \text{ mV} \cdot \text{s}^{-1}$ . The PC ( $\sigma$ ) of the IPMC membrane was evaluated using the following formula [14]:

$$\sigma = \frac{L}{R \times A} \quad (4)$$

where  $\sigma$ ,  $L$ ,  $R$ , and  $A$  are the PC, thickness (in cm), resistance (in ohm), and cross-sectional area (in  $\text{cm}^2$ ) of the studied IPMC membrane.

### 2.2.11. Electromechanical Characterization

In order to find the electromechanical properties of the KR-CuNPs-Pt polymer soft actuator, a test setup was established, and the basic layout for actuation and control of the actuator is shown in Figure 1. The actuator was fixed in a holder mounted in a cantilever mode. A laser-based displacement sensor was taken to get the displacement after feedback while finding the displacement of the actuator at the tip end. This provides feedback during the operation of the actuator. The successive bending responses after providing the different voltages are shown in Figure 2. The tip deflection data of the actuator is provided in Table 1. The size of  $30 \text{ mm} \times 10 \text{ mm} \times 0.2 \text{ mm}$  for the actuator was taken during experimentation. The bi-directional deflection behavior of the actuator is also plotted, as shown in Figure 3. For obtaining the deflection/displacement behavior, the voltage (4 VDC) was supplied to the actuator using a digital power supply and digital-analog card (DAC) where the electrical pulse is sent through command control operation. For controlling the voltage, a basic software of digital-analog card was used where input command is sent by providing voltage up to 4 DC. When applying voltage (4 VDC), the straight behavior was achieved (ca. 18.2 mm), whereas at 3.5 VDC, the deflection of ca. 14.8 mm was achieved after several trials, as shown in Figure 3. It is envisaged that the bi-directional deflection behavior of the polymer actuator has some amount of hysteresis. The experiments were also repeated, and it was found that the hysteresis behaviors show that the tip deflection of the actuator increased with increasing of the voltage. Bi-directional deflection behavior of the actuator does not attend the exact behavior and has a deflection error (i.e., hysteresis), which is overcome by setting up the voltage in DAC while controlling the actuation process of the actuator. It shows the repeatable behavior within the deflection range up to ca. 18.2 mm (maximum).

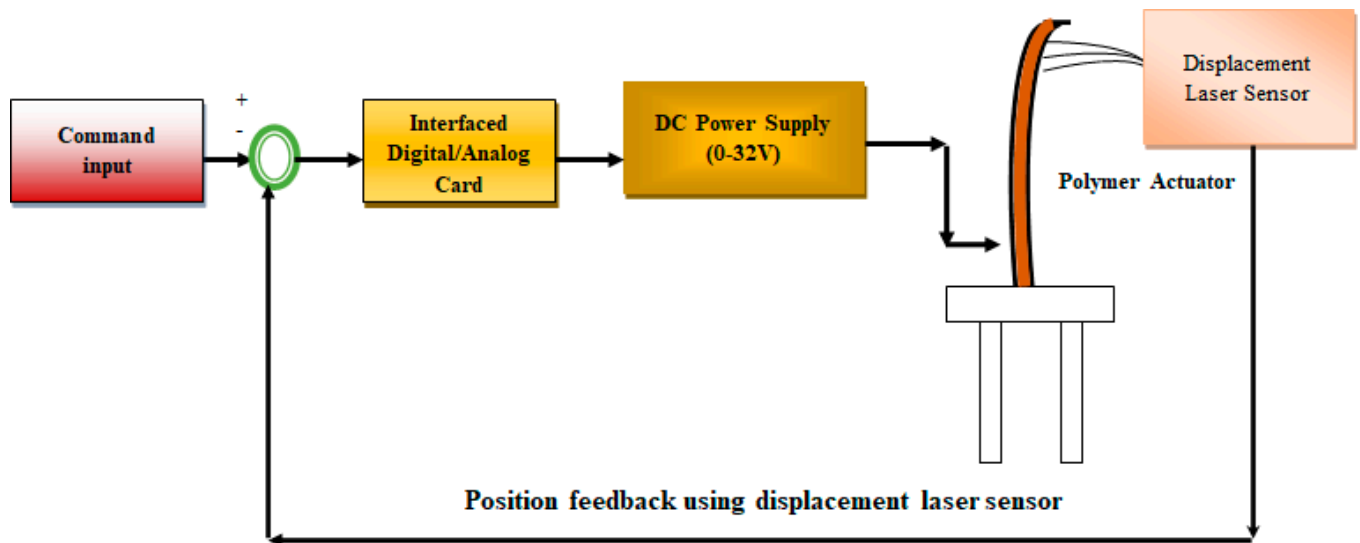


Figure 1. Basic layout for actuation and control of the KR-CuNPs-Pt polymer actuator.

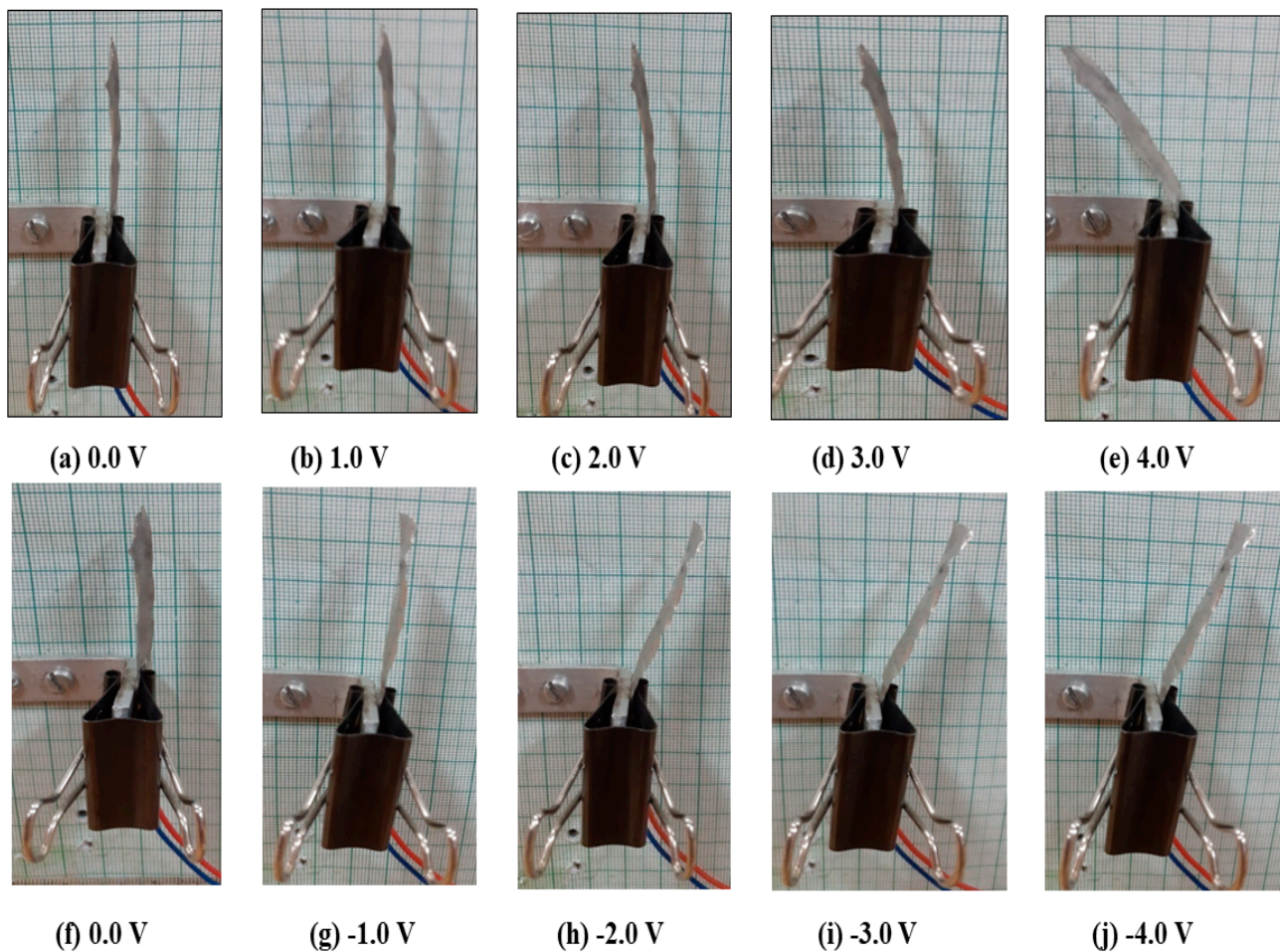
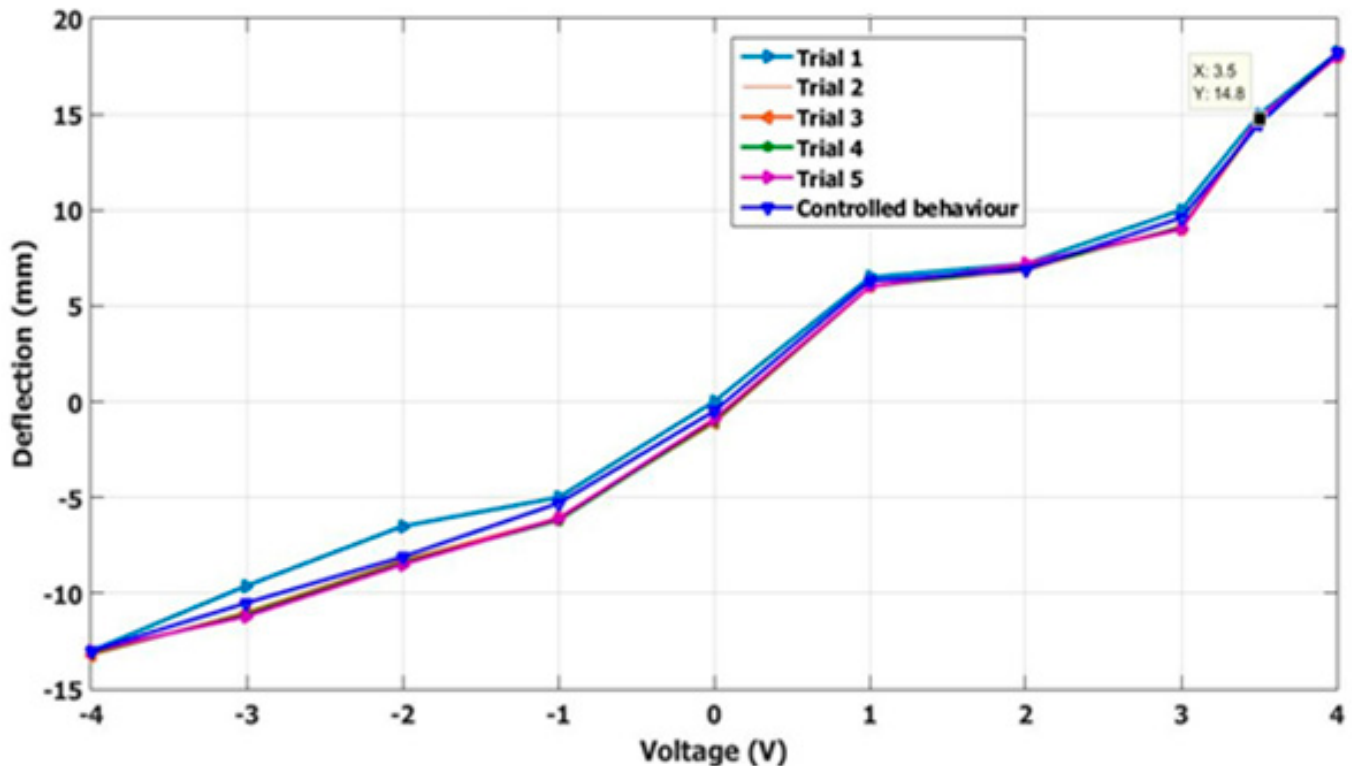


Figure 2. Step-by-step bi-directional deflection behavior of the KR-CuNPs-Pt actuator.

**Table 1.** Deflection data (experimental) of the KR-CuNPs-Pt polymer soft actuator.

Voltage	Deflection (In mm)				
	0.0 V	1.0 V	2.0 V	3.0 V	4.0 V
Trial 1	0	5.5	7.0	9.1	18.0
Trial 2	0	6.0	7.1	9.0	18.1
Trial 3	0	5.8	7.2	9.2	18.0
Trial 4	0	6.1	7.0	9.0	18.2
Trial 5	0	6.2	7.5	9.4	18.1

**Figure 3.** Deflection behavior of the KR-CuNPs-Pt polymer actuator obtained experimentally.

### 3. Result and Discussion

#### 3.1. FTIR Spectra

Figure 4a,b represents the FTIR spectra of the studied KR-CuNPs and KR-CuNPs-Pt IPMCs membranes. The spectrum of the KR-CuNPs polymer membrane shows a broad absorption peak at  $3432\text{ cm}^{-1}$  due to the stretching mode assigned to the  $-\text{OH}$  group of the sulfonic acid group, while the absorption peaks at  $2918$  and  $2864\text{ cm}^{-1}$  were obtained due to C-H stretching modes of  $-\text{CH}_2$  and  $-\text{CH}_3$  groups [21]. The characteristic absorption peaks at  $1032$  and  $1024\text{ cm}^{-1}$  belonging to S=O bonds stretch for sulfonate groups attached to the polymeric chains were also seen. The peaks correspond at  $1622\text{ cm}^{-1}$  for C=C stretching vibration of the benzenoid ring, and  $590\text{ cm}^{-1}$  corresponds to the presence of Cu-metal at the surface of the membrane. Nevertheless, it was seen that the increase in the intensity of adsorption peaks was due to an increase in the sulfonate group owing to the concentrated sulfuric acid. FTIR studies of the KR-CuNPs-Pt IPMCs membranes (Figure 4b) revealed that a strong peak near  $520\text{ cm}^{-1}$  contributed to the vibration of Pt-metal, which indicates the successful coating carried out at the surface of the membrane. Figure 4b shows all the vibrations with less intensity, similar to those in Figure 4a.

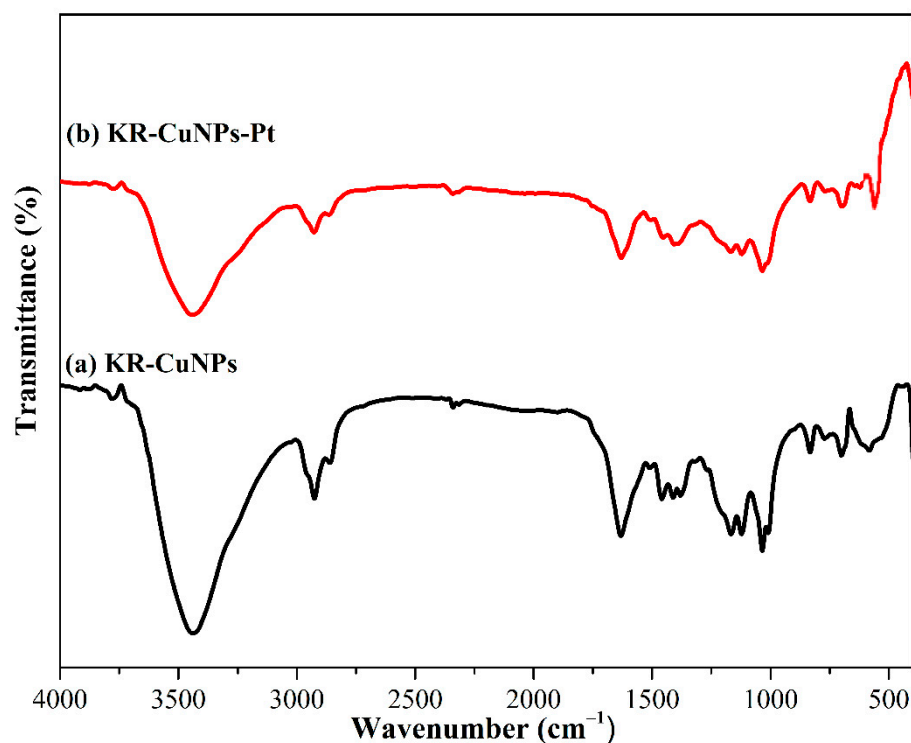


**Figure 4.** FTIR spectra of (a) KR-CuNPs and (b) KR-CuNPs-Pt IPMCs membranes.

### 3.2. IEC, PC, WU and WL

The IEC of the ionomers has a great influence on facilitating proton transfer in the hydrated IPMCs membrane, and, thus, helps in high performance of actuators. The IEC of the studied KR-CuNPs-Pt IPMC membrane was evaluated and found to be ca.  $2.10 \text{ meq}\cdot\text{g}^{-1}$ . The high IEC value of the IPMC membrane led to an increase in the WU capacity and allowed more Pt-particles to intensely fix on both sides of the surfaces of the membrane. The uniform electrode and more Pt-particles on the surface of membrane will reduce the resistance of IPMCs, and hence establish an excellent bending performance [22,23]. With the temperature increase, the membrane's WU capacity increases. Table 2 shows the maximum WU capacity of the membrane at RT ( $25 \pm 1 \text{ }^\circ\text{C}$ ),  $45 \text{ }^\circ\text{C}$ , and  $65 \text{ }^\circ\text{C}$  for 1 h of immersion time and it was found to be ca. 48.5, 59.62, and 71.05%, respectively. It was seen that a gradual decrease in the water holding capacity as the immersion time increases, till almost 25 h, where it gets almost stabilized, which is plotted in Figure 5. Water absorption at a higher temperature was not tried as it will be near ( $\sim 100 \text{ }^\circ\text{C}$ ) to the Styrene glass transition temperature of the Styrene, one of the blocks of the Kraton. We have tried three different temperatures to balance water absorption levels and stable mechanical membranes. The high WU capacity of the membrane indicates the increasing hydrophilic nature, which is expected to help in better performance under an applied potential. The WL, through the damage of the electrode layer and electrolysis of water of the membrane, is a negative factor for the performance of an IPMC actuator. Hence, WL capacity was performed for the membrane with highest water uptake level after applying electric potentials (3–6 V). It is seen from Figure 6 that the membrane lost water to some extent due to electrolysis, and this caused the damage to the electrode layer via the creation of pores on the surface of the electrode. It is observed that the WL from the membrane increases with an increase in the applied voltage and that the maximum loss is ca. 38% at 6 V for 9 min. The slow and low level of WL is a good indication for a better membrane performance. The precision of the KR-CuNPs-Pt IPMC membrane was checked toward the WU and WL capabilities; the experiments were repeated five times at room temperature ( $25 \pm 1 \text{ }^\circ\text{C}$ ) and  $65 \text{ }^\circ\text{C}$ . The average values of five experiments were taken to plot an error bar of WU and WL

(Figures 7 and 8). From this error bar, it is clear that there is no significant change in the WU and WL capacities after the same experiment was repeated.

**Table 2.** IEC, PC, and WU of the KR-CuNPs IPMCs membrane.

Materials	IEC (meq·g <sup>-1</sup> )	$\sigma$ (mS·cm <sup>-1</sup> )	WU (%)		
			at RT	at 45 °C	at 65 °C
KR-CuNPs	2.10	1.93	48.5 (1 h)	59.62 (1 h)	71.05 (1 h)

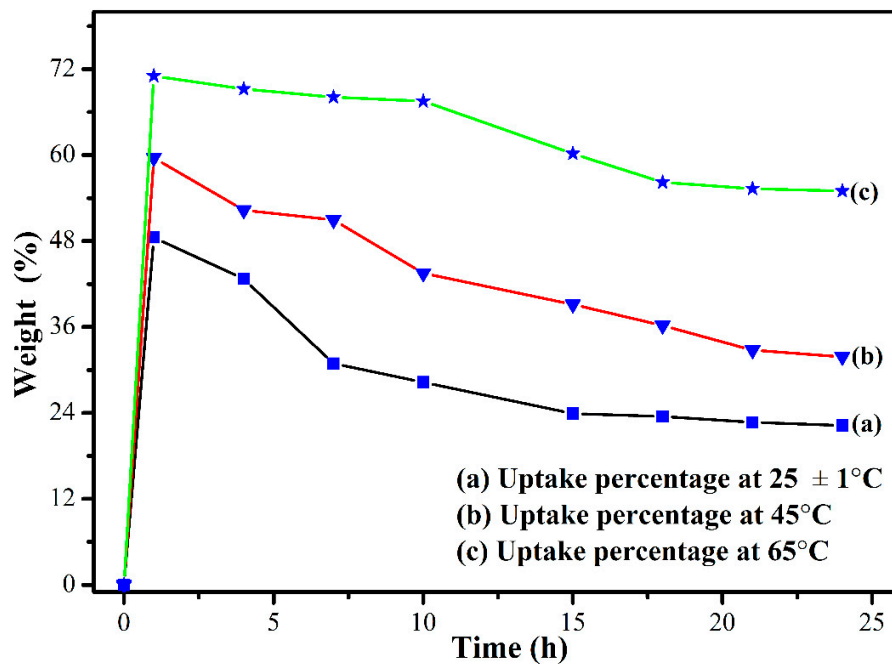


**Figure 5.** Water uptake of the KR-CuNPs membrane at 25, 45, and 65 °C at different intervals of time.

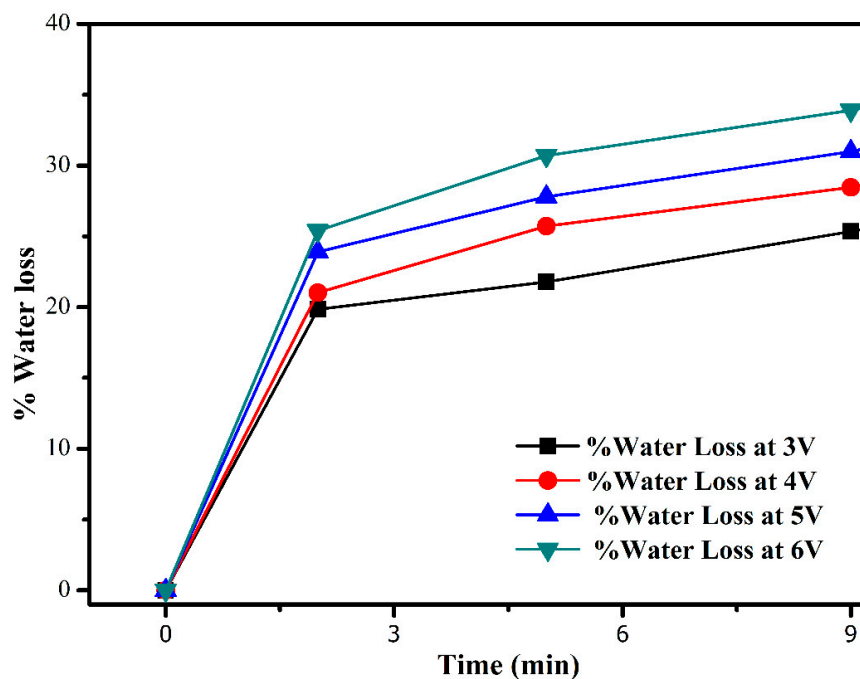


**Figure 6.** Water loss of the KR-CuNPs-Pt IPMCs membrane at 3–6 V.

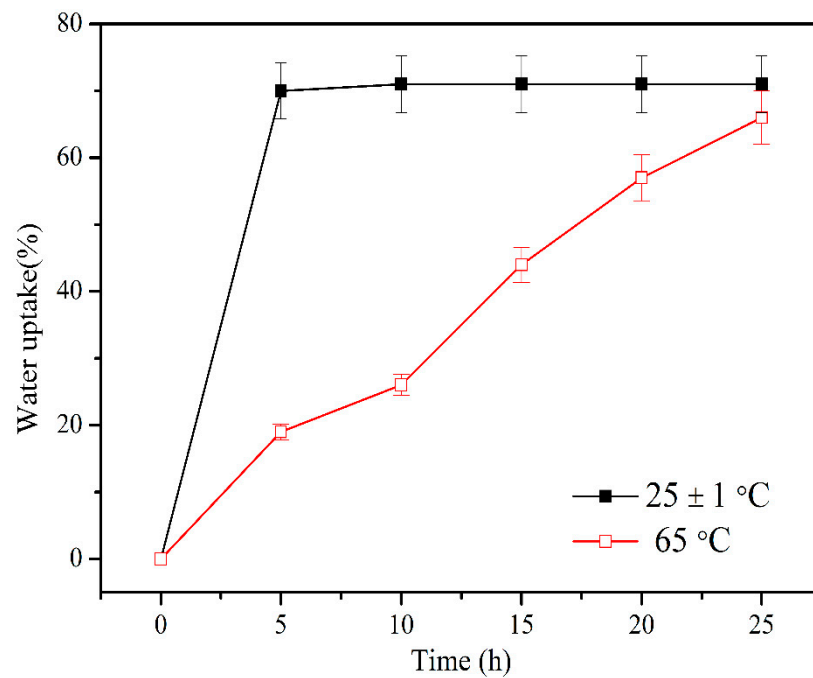


Figure 7. Error bar for WU of the KR-CuNPs-Pt membrane.

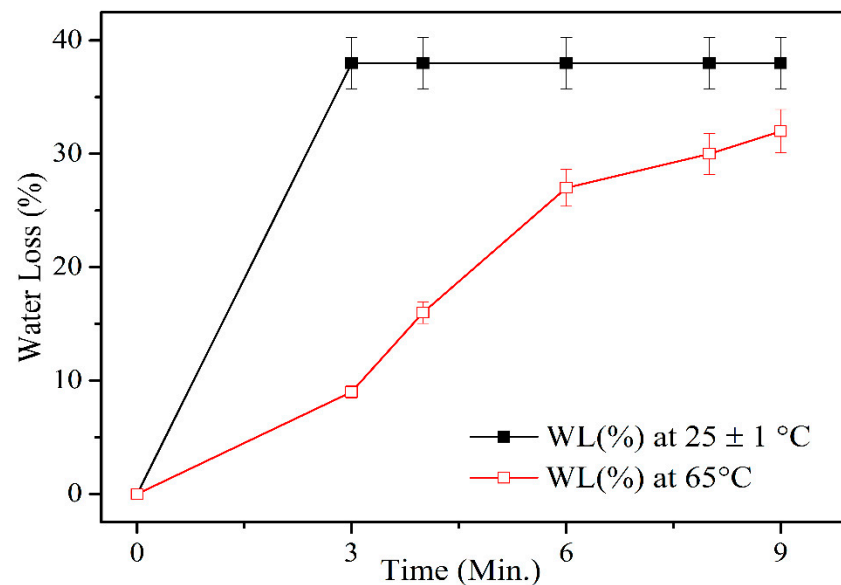


Figure 8. Error bar for WL of the KR-CuNPs-Pt membrane.

The PC of IPMC membrane was found to be  $1.93 \text{ mS}\cdot\text{cm}^{-1}$ . A high value of PC facilitates the migration of excess  $\text{H}^+$  ions in their hydrated form, which facilitates enhanced actuation capacity.

### 3.3. SEM Study

SEM images describe the surface and cross-sectional morphology of the KR-CuNPs-Pt membrane, and these were applied to identify the distribution of Pt-metal, dispersion of KR and CuNPs, and coating at the porous surface of the membrane, shown in Figure 9a–d. Figure 9a,b represents the surface morphology of the membrane at magnification  $500\times$  and  $5000\times$ , respectively, while Figure 9c,d exhibits the cross-sectional view of the membrane at the same ( $300\times$ ) magnification. The smooth shining at the porous texture of self-assembled chains of the membrane confirms the coating of Pt at the surface of the membrane. There-

fore, the images confirm the successful synthesis of the KR-CuNPs membrane and coating using Pt-metal. Such morphology can also be confirmed for their cross-sectional images of the membrane.

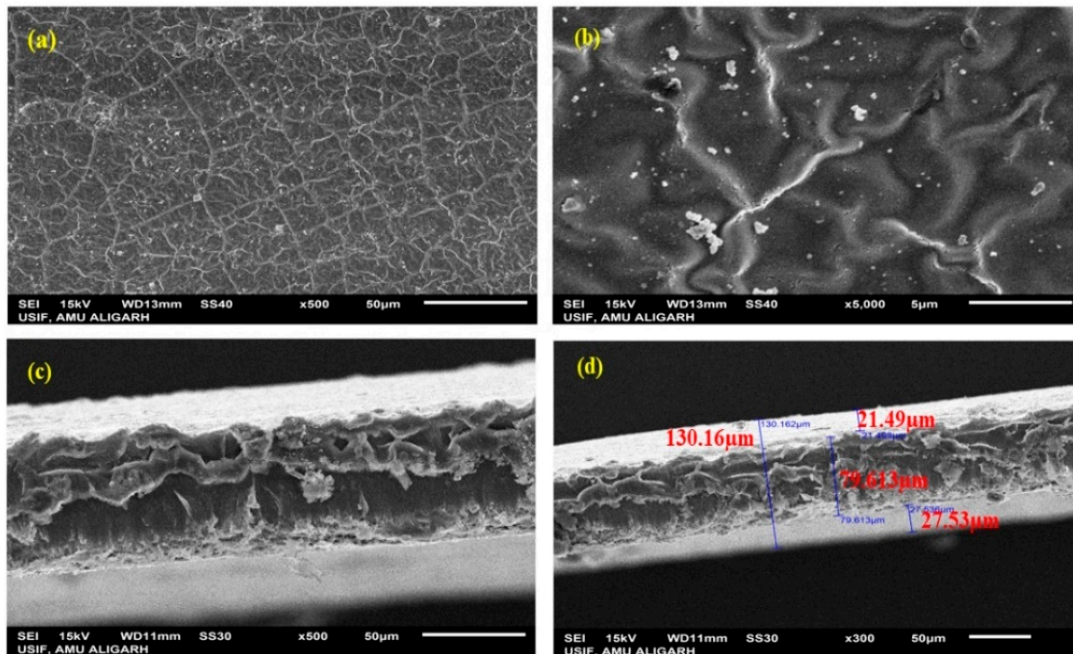


**Figure 9.** SEM images of (a,b) KR-CuNPs-Pt at resolutions  $500\times$  and  $5000\times$ , (c,d) are cross-sectional views of the KR-CuNPs-Pt composite-based membrane.

### 3.4. EDX Study

EDX image of the studied KR-CuNPs-Pt membrane can be seen in Figure 10. The spectrum obtained for the membrane reveals the presence of elements such as carbon (C), copper (Cu), sulphur (S), and platinum (Pt) at the surface of the actuator. The surface of the membrane shows the characteristic spectrum of the elements present in the membrane. The highest percentage of Pt confirms an excellent coating of the metal electrode at the surface of the KR-CuNPs-Pt membrane actuator.

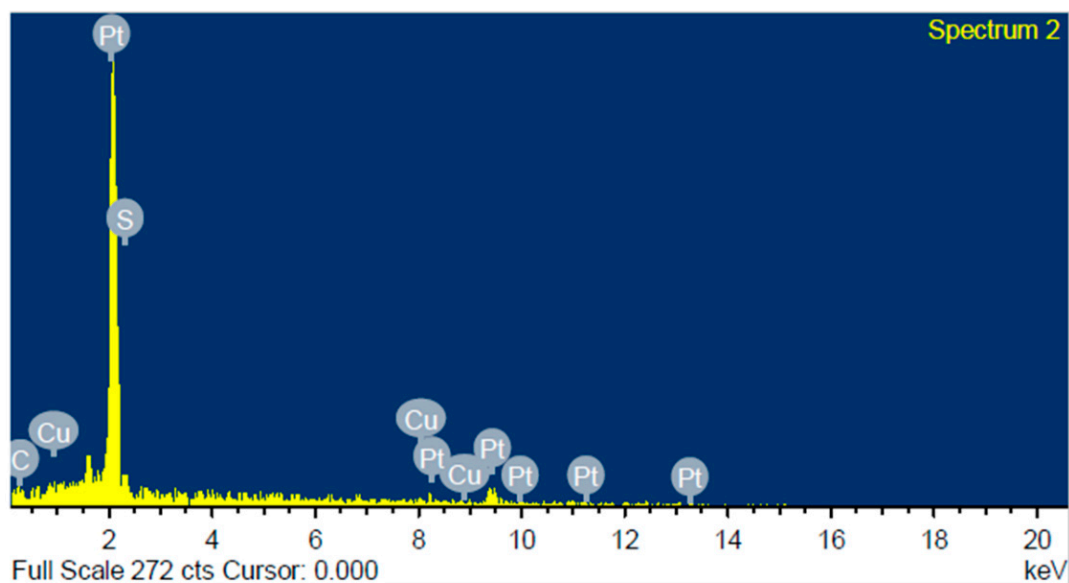


**Figure 10.** EDX graph of the KR-CuNPs-Pt IPMC membrane.

### 3.5. X-ray Diffraction (XRD) Patterns Study

Figure 9a–c describes the XRD patterns of studied CuNPs, KR-CuNPs, and KR-CuNPs-Pt IPMCs membranes. Four different diffraction peaks are observed at  $2\theta$  values of ca.  $35.8^\circ$  and  $38.58^\circ$  for  $\text{Cu}_2\text{O}$ , and ca.  $43.2^\circ$  and  $50.6^\circ$  for CuNPs in Figure 11a,b. Figure 11c describes the XRD pattern of the KR-CuNPs-Pt, exhibiting the characteristic properties of crystalline Pt face-centered cubic (fcc) lattice. The peaks were characterized (111) peaks firstly, and the next (200) and (220) peaks to the  $2\theta$  value of ca.  $39.45^\circ$ ,  $45.96^\circ$ , and  $67.36^\circ$ , respectively. The relative sharpness of observed peaks may be associated with an increase in the crystalline structures of the studied polymer membranes due to H-bonding to the sulfonic groups, causing alignment of polymer chains. Blending of KR-CuNPs to Pt, the patterns of XRD peaks of the prepared KR-CuNPs-Pt IPMC membrane revealed similar diffraction peaks for the Kraton. These investigations of the XRD spectra exhibit an amorphous nature of the KR-CuNPs-Pt IPMCs membrane [24,25].

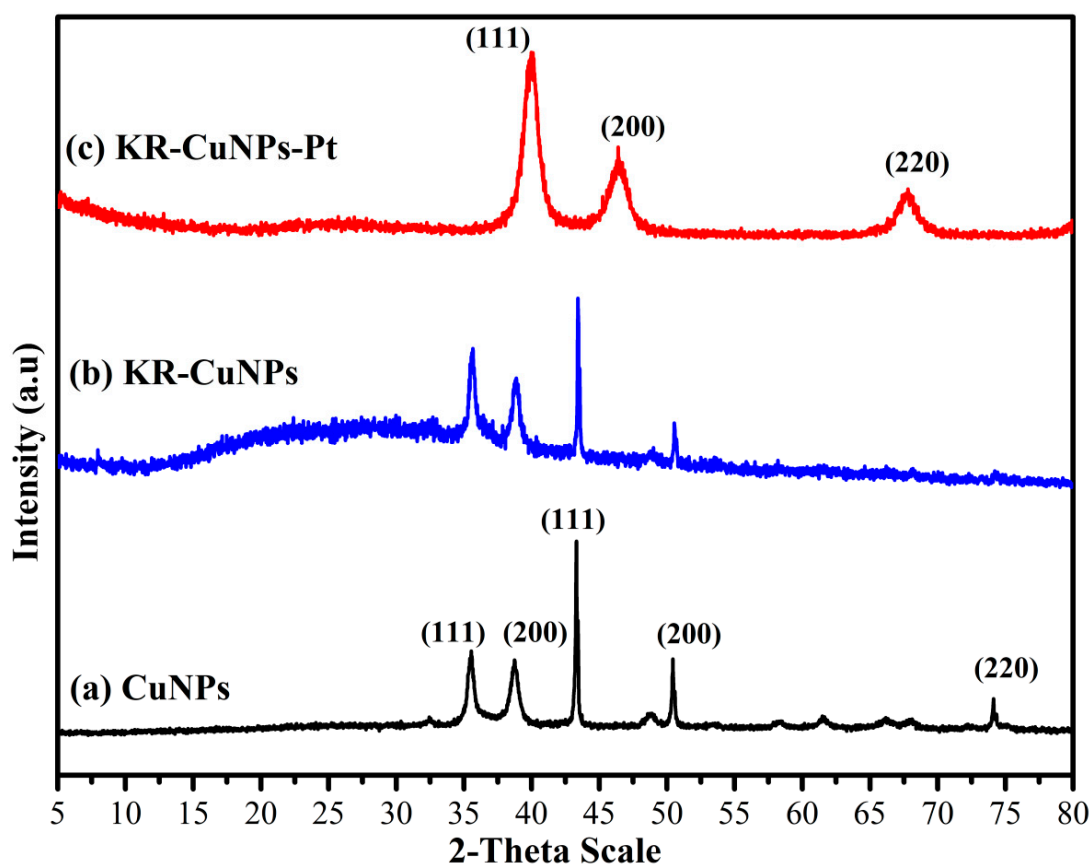


**Figure 11.** XRD spectrum of (a) CuNPs, (b) KR-CuNPs, and (c) KR-CuNPs-Pt IPMC membranes.

### 3.6. TEM Study

The characterization of the prepared IPMC membrane to show the particle size was performed through TEM study, and the micrographs are shown in Figure 12a,b. The homogeneous distribution of Pt metal can be seen in Figure 12a. After blending Pt with KR and CuNPs ion-exchange polymers, the Pt layers stack together to form a composite structure, as shown in Figure 12b. It can be clearly seen that Pt is homogeneously blended and covers the background of the membrane matrix, to a large extent confirming the homogeneous blending of composite KR, CuNPs, and Pt in the fabricated IPMC membrane. The average particle size was calculated to ca. 19 nm (Figure 12b).

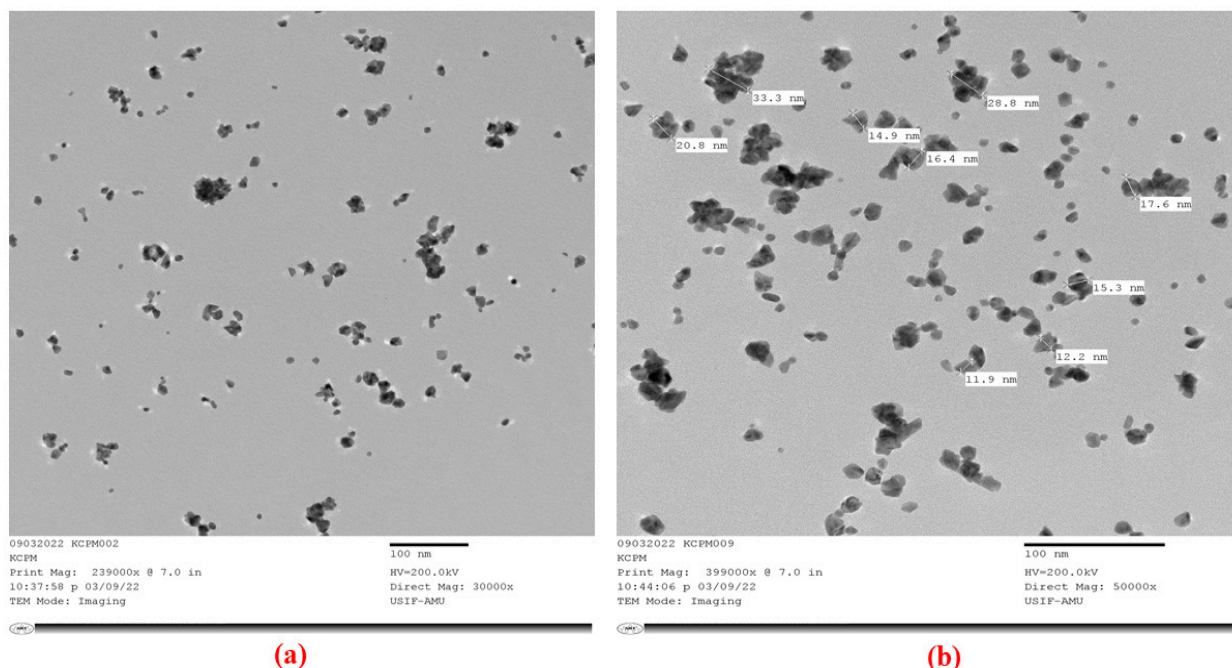


**Figure 12.** TEM micrographs of (a) KR-CuNPs-Pt IPMC membrane and (b) with average particle size of Pt in the membrane.

3.7. Electromechanical Characterization

The actuation force behavior of the KR-CuNPs-Pt polymer actuator was characterized to study its electromechanical approach. The polymer actuator was held in the mechanical fixture as discussed in Section 2.2.11. A digital weighing scale was used for measuring the force of the actuator. The voltage (0–4 VDC) was applied to the actuator. During applying the voltage (0–4 VDC), the actuator touched a pan of the digital weighing scale. The force values were noted and are summarized in Table 3. It was observed that the maximum force that this soft actuator can attain is ca. 0.343 mN, as shown in Figure 13. A normal distribution curve was also drawn, as shown in Figure 14. It has a narrow shape, and, thus, shows a low level of error and good repeatability behavior of the force characteristics at the applied voltage. The repeatability of this polymer actuator was ca. 86.295%.

**Table 3.** Force data of the KR-CuNPs-Pt polymer soft actuator.

Voltage (V)	F1 (mN)	F2 (mN)	F3 (mN)	F4 (mN)	F5 (mN)	Average Force Value (F) in mN
0	0	0	0	0	0	0
1	0.042	0.04	0.041	0.042	0.042	0.0414
2	0.102	0.103	0.104	0.103	0.102	0.1028
3	0.292	0.292	0.292	0.291	0.292	0.2918
4	0.345	0.342	0.341	0.344	0.345	0.3434
		Mean				0.155
		Standard Deviation				0.137
		Repeatability				86.295%

A KR-CuNPs-Pt soft actuator-based micro gripping system was developed, as shown in Figure 15. The two soft actuators are held in the holder where the voltage (4 VDC) is applied to each polymer actuator and is given to the opposite polarity of the voltage so that the gripping concept is achieved. This gripper can hold a light weight (ca. 8.5 mg) object (15 × 15 mm<sup>2</sup>) based on thermocol. This shows the potential of micro-robotic applications using a developed soft polymer actuator.

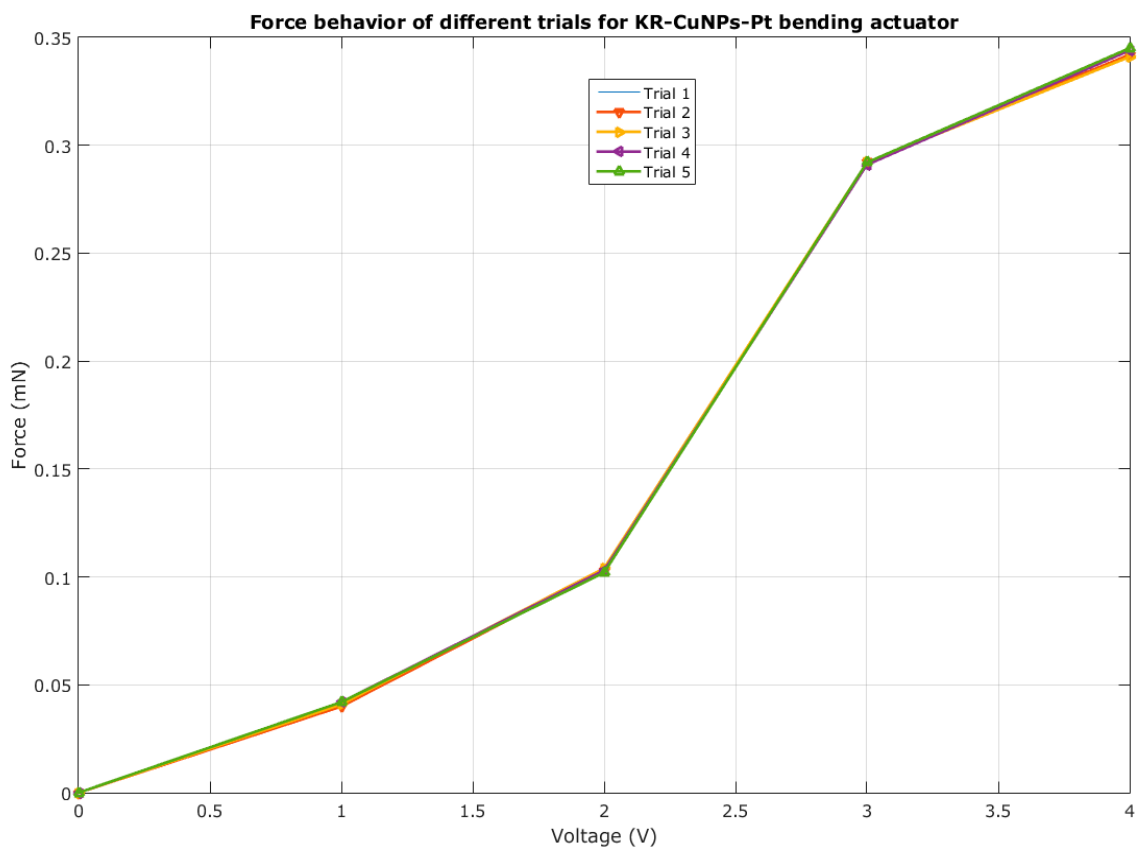


Figure 13. Force behavior of different trials for the KR-CuNPs-Pt bending actuator.

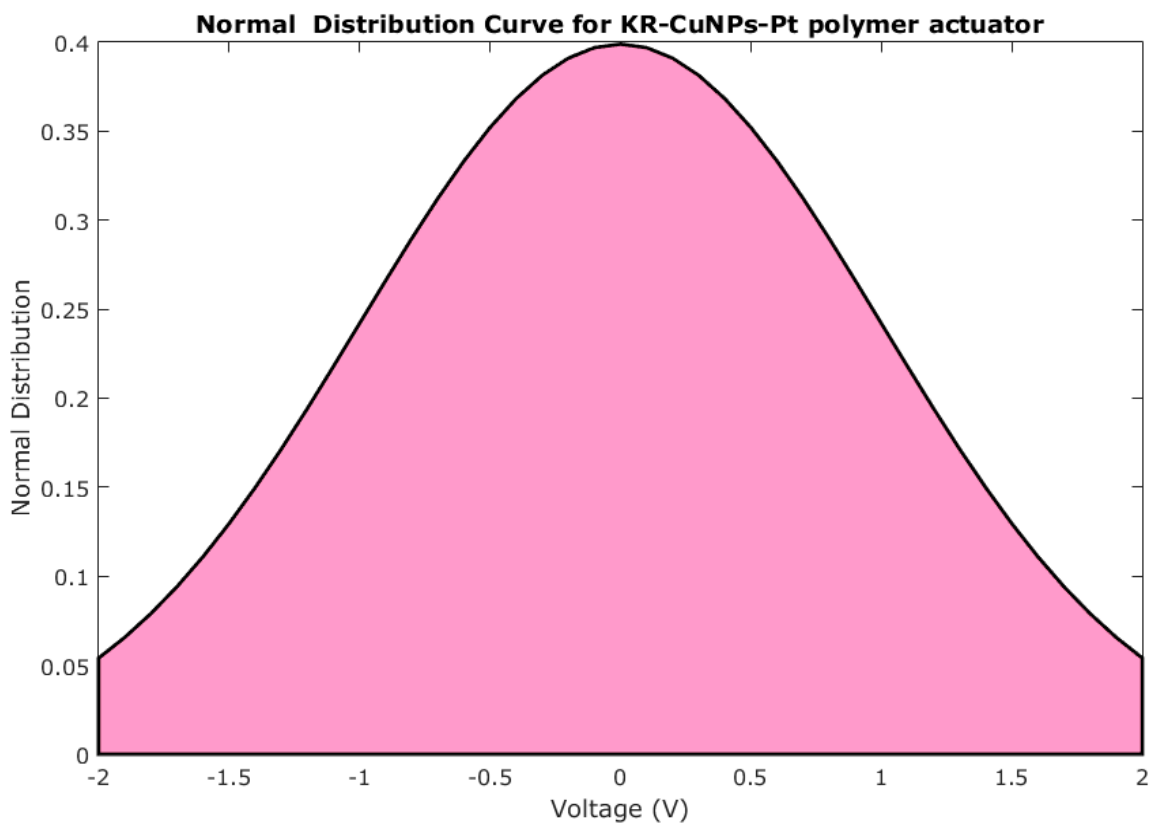


Figure 14. Normal distribution behavior of the KR-CuNPs-Pt bending actuator.



**Figure 15.** A KR-CuNPs-Pt soft actuators-based micro gripping system.

#### 4. Conclusions

The current article presents the development of novel Kraton-based KR-CuNPs-Pt IPMC membranes. The membranes were characterized using various physical, structural, morphological, and electromechanical study techniques. The high PC ( $\sigma$ ), IEC, WU capacity, good repeatability, and slow and low level of WL under applied electric potential provide a good performance of the developed membrane. Electromechanical studies (actuation force and tip displacement/deflection) reveal an excellent bending response of the studied IPMC membrane. A micro-gripper was also developed, showing that the developed IPMC polymer actuator membrane can be applied for soft robotic applications. These results exhibit that the incorporation of CuNPs can be helpful in making cost effective IPMC membranes by replacing to some extent the expensive Pt-metal on both sides of the membrane, serving as electrode layers. Hence, the developed novel KR-CuNPs-Pt based actuator is a promising material that may be utilized in micro-robotic applications, including micro gripper, bioengineering, and biologically-inspired robotic systems.

**Author Contributions:** Conceptualization, M.L., H.M.S. and A.A.; methodology, M.L., H.M.S. and A.A.; formal analysis, H.M.S., A.A. and M.A.A.; investigation, M.L., H.M.S. and A.A.; resources, S.M.A.-Z. and M.L.; writing—original draft preparation, M.L. and A.A.; writing—review and editing, M.L., A.A. and H.M.S.; supervision, S.M.A.-Z.; funding acquisition, M.L. and H.M.S. All authors have read and agreed to the published version of the manuscript.

**Funding:** This project was funded by the National Plan for Science, Technology and Innovation (MAARIFAH), King Abdulaziz City for Science and Technology, Kingdom of Saudi Arabia, Award Number (13-ADV1432-02).

**Institutional Review Board Statement:** Not applicable.

**Informed Consent Statement:** Not applicable.

**Data Availability Statement:** Data are contained within the article.

**Conflicts of Interest:** The authors declare no conflict of interest.

## References

1. Ionov, L. Polymeric Actuators. *Langmuir* **2005**, *31*, 5015–5024. [[CrossRef](#)] [[PubMed](#)]
2. Luqman, M.; Anis, A.; Shaikh, H.M.; Al-Zahrani, S.M.; Alam, M.A. Development of a Soft Robotic Bending Actuator Based on a Novel Sulfonated Polyvinyl Chloride–Phosphotungstic Acid Ionic Polymer–Metal Composite (IPMC) Membrane. *Membranes* **2022**, *12*, 651. [[CrossRef](#)]
3. Luqman, M.; Shaikh, H.M.; Anis, A.; Al-Zahrani, S.M.; Alam, M.A. A convenient and simple ionic polymer-metal composite (IPMC) actuator based on a platinum-coated sulfonated poly(ether ketone)–polyaniline composite membrane. *Polymers* **2022**, *14*, 668. [[CrossRef](#)]
4. Turner, A.J.; Ramsay, K. Review and development of electromechanical actuators for improved transmission control and efficiency. *SAE Tech. Pap.* **2004**, *113*, 908–919. [[CrossRef](#)]
5. Luqman, M.; Shaikh, H.; Anis, A.; Al-Zahrani, S.M.; Hamidi, A.; Inamuddin. Platinum-coated silicotungstic acid-sulfonated polyvinyl alcohol-polyaniline based hybrid ionic polymer metal composite membrane for bending actuation applications. *Sci. Rep.* **2022**, *12*, 4467. [[CrossRef](#)]
6. Ahamed, M.I.; Asiri, A.M.; Luqman, M. Preparation, physicochemical characterization, and microrobotics applications of polyvinyl chloride-(PVC-) based PANI/PEDOT: PSS/ZrP composite cation-exchange membrane. *Adv. Mater. Sci. Eng.* **2019**, *2019*, 4764198. [[CrossRef](#)]
7. Saint Martin, L.B.; Mendes, R.U.; Cavalca, K.L. Electromagnetic actuators for controlling flexible cantilever beams. *Struct. Control. Health Monit.* **2018**, *25*, e2043. [[CrossRef](#)]
8. Xu, J.M.; Ma, L.; Han, H.L.; Ni, H.Z.; Wang, Z.; Zhang, H.X. Synthesis and properties of a novel sulfonated poly(arylene ether ketone sulfone) membrane with a high  $\beta$ -value for direct methanol fuel cell applications. *Electrochim. Acta* **2014**, *146*, 688–696. [[CrossRef](#)]
9. Kim, K.J.; Shahinpoor, M. Ionic polymer–metal composites: II. *Manufacturing techniques*. *Smart Mater Struct.* **2003**, *12*, 65–79. [[CrossRef](#)]
10. Ru, C.Y.; Gu, Y.Y.; Duan, Y.T.; Zhao, C.J.; Na, H. Enhancement in proton conductivity and methanol resistance of Nafion membrane induced by blending sulfonated poly(arylene ether ketones) for direct methanol fuel cells. *J. Membr. Sci.* **2019**, *573*, 439–447. [[CrossRef](#)]
11. Inamuddin; Khan, A. An overview of preparation, properties and applications of ionic polymer composite actuators. In *New Polymeric Composite Materials: Environmental, Biomedical, Actuator and Fuel Cell Applications*; Inamuddin, Mohammad, A.I., Asiri, M.A., Eds.; Materials Science Forum Scientific: Millersville, PA, USA, 2016; Volume 11, pp. 326–386.
12. Khan, A.; Jain, R.K.; Asiri, A.M. Thorium (IV) phosphate-polyaniline composite-based hydrophilic membranes for bending actuator application. *Polym. Eng. Sci.* **2017**, *57*, 258–267. [[CrossRef](#)]
13. Khan, A.; Jain, R.K.; Luqman, M.; Asiri, A.M. Development of sulfonated poly(vinyl alcohol)/aluminium oxide/graphene based ionic polymer-metal composite (IPMC) actuator. *Sens. Actuators A Phys.* **2018**, *280*, 114–124. [[CrossRef](#)]
14. Khan, A.; Jain, R.K.; Banerjee, P.; Ghosh, B.; Asiri, A.M. Development, characterization and electromechanical actuation behavior of ionic polymer metal composite actuator based on sulfonated poly(1,4-phenylene ether-ether-sulfone)/carbon nanotubes. *Sci. Rep.* **2018**, *8*, 9909. [[CrossRef](#)] [[PubMed](#)]
15. Inamuddin; Khan, A.; Jain, R.K.; Naushad, M. Development of sulfonated poly(vinyl alcohol)/polypyrrole based ionic polymer metal composite (IPMC) actuator and its characterization. *Smart Mater. Struct.* **2015**, *24*, 095003. [[CrossRef](#)]
16. Khan, A.A.; Inamuddin; Alam, M.M. Determination and separation of Pb<sup>2+</sup> from aqueous solutions using a fibrous type organic-inorganic hybrid cation exchange material: Polypyrrole thorium(IV) phosphate. *React. Funct. Polym.* **2005**, *63*, 119–133. [[CrossRef](#)]
17. Khan, A.; Inamuddin; Jain, R.K.; Naushad, M. Fabrication of a silver nano powder embedded kraton polymer actuator and its characterization. *RSC Adv.* **2015**, *5*, 91564. [[CrossRef](#)]
18. Patil, S.A.; Ryu, C.H.; Kim, H.S. Synthesis and characterization of copper nanoparticles (Cu-Nps) using rongalite as reducing agent and photonic sintering of Cu-Nps ink for printed electronics. *Int. J. Precis. Eng. Manuf.-Green Technol.* **2018**, *5*, 239–245. [[CrossRef](#)]
19. Jain, R.K.; Khan, A.; Inamuddin; Asiri, A.M. Design and development of non-perfluorinated ionic polymer metal composite-based flexible link manipulator for robotics assembly. *Polym. Compos.* **2019**, *40*, 2582–2593. [[CrossRef](#)]
20. Luqman, M.; Lee, J.W.; Moon, K.K.; Yoo, Y.T. Sulfonated polystyrene-based ionic polymer–metal composite (IPMC) actuator. *J. Ind. Eng. Chem.* **2011**, *17*, 49–55. [[CrossRef](#)]
21. Khan, A.; Jain, R.K.; Banerjee, P.; Inamuddin; Asiri, A.M. Soft actuator based on Kraton with GO/Ag/Pani composite electrodes for robotic applications. *Mater. Res. Express.* **2017**, *4*, 115701. [[CrossRef](#)]
22. Inamuddin; Jain, R.K.; Hussain, S.; Naushad, M. Poly(3,4-ethylenedioxythiophene): Polystyrene sulfonate zirconium(IV) phosphate (PEDOT:PSS-ZrP) composite ionomeric membrane for artificial muscle applications. *RSC Adv.* **2015**, *5*, 84526–84534. [[CrossRef](#)]

23. Khan, A.; Inamuddin; Jain, R.K. Easy, operable ionic polymer metal composite actuator based on a platinum-coated sulfonated poly(vinyl alcohol)–polyaniline composite membrane. *J. Appl. Polym. Sci.* **2016**, *133*, 43787. [[CrossRef](#)]
24. Inamuddin; Khan, A.; Luqman, M.; Dutta, A. Kraton based ionic polymer metal composite (IPMC) actuator. *Sens. Actuators A Phys.* **2014**, *216*, 295–300. [[CrossRef](#)]
25. Jain, R.K.; Majumder, S.; Dutta, A. SCARA based peg-in-hole assembly using compliant IPMC micro gripper. *Rob. Auton. Syst.* **2013**, *61*, 297–311. [[CrossRef](#)]